Desalination and Water Treatment
www.deswater.com

doi:10.5004/dwt.2019.24510

165 (2019) 374–381
October

Synthesized nano titanium for Methylene Blue removal under various operational conditions

Mahmoud Samy, Mohamed Mossad*, Hisham Kh. El-Etriby

Public Works Department, Faculty of Engineering, Mansoura University, Egypt, email: mahmoud.3zzab@gmail.com (M. Samy), Tel. +201097116633, email: maahm@mans.edu.eg (M. Mossad), eletriby@mans.edu.eg (H. El-Etriby)

Received 1 March 2019; Accepted 8 June 2019

ABSTRACT

In this study, photo-catalytic degradation of methylene blue (MB) in aqueous solution by using synthesized nano TiO_2 prepared by sol-gel method was investigated under various operational conditions (catalyst dose, pH of the solution, initial concentration of dye and illumination time). Full characterization of the synthesized nano titanium was carried out. SEM and FTIR before and after degradation demonstrated the interaction between MB dye and TiO_2. The synthesized TiO_2 band gap falls in the visible light region which demonstrates the activation of TiO_2 in visible light and enhances its removal efficiency. Photo-degradation efficiency of MB was strongly influenced by the operational parameters. The photo-degradation efficiency decreased with increasing the initial concentration of MB. Alkaline media is favorable for photo-catalytic degradation due to high adsorption of MB molecules into the catalyst. The photo-catalytic reactions followed pseudo-first order kinetics and the reaction rate was inversely related to the feed concentrations.

Keywords: Photocatalysis; Methylene blue; Titanium dioxide; Photodegradation; Operational parameters

1. Introduction

Dyes are abundant class of colored organic compounds which are widely used as colorants in many industries such as leather tanning, textile,paper, plastic, pharmaceutical [1]. Dyes are one of the most serious contaminates for wastewater because of their toxicity and carcinogenic properties [2]. Many techniques have been applied for dyes removal from industrial wastewater such as flocculation, adsorption, air stripping, precipitation, reverse osmosis, ion exchange, ultrafiltration and advanced oxidation processes [1,3]. Most of those techniques are not cost effective since they only transfer the non-biodegradable matter into sludge, which require further treatment [4,5]. Advanced oxidation processes (AOPs) and adsorption are the most effective technologies for dyes removal and other complex organic from industrial wastewater [6,7]. Semiconductor photo-catalysis is an important destructive technology that achieves complete mineralization of most resistant organic pollutants [8]. There are many different types of semiconductors that can be used as photo-catalysts such as (TiO_2, ZnO, WO_3, CdS, GaAS, PbS). Among those semiconductors photo-catalysts, titanium dioxide (TiO_2) has been proven to be the most convenient for widespread environmental applications due to its biological and chemical inertness, strong oxidizing power, ease of preparation, commercially available, nontoxicity, water insolubility and long-term stability against photo-corrosion [9–11]. In photo-catalysis process, TiO_2 is excited by photons having an energy level that exceeds its band gap. Consequently, electrons are excited from the valence band to the conduction band forming an electron/hole pair (e^-/h^+). The valence band (h^+) reacts with water or hydroxide ion (OH^-) adsorbed on the catalyst surface to form hydroxyl radicals ($OH^\cdot$) which are strong oxidant and the conduction band (e^-) reacts with oxygen to form super-oxide oxygen. Organic pollutants on or near the surface of TiO_2 will be attacked and oxidized by hydroxyl radical. It causes decomposition of toxic and

*Corresponding author.

bio-resistant compounds into harmless species such as CO_2, H_2O [12–15]. Many researchers prepared nano sized TiO_2 by sol-gel method [10,11,16]. Most band gap of synthesized nano sized TiO_2 photo-catalyst falls in the UV light region [10]. Baker et al. prepared nano titanium by sol gel method which has a band gap of 3.19 that approached to the visible light region (388 nm) [11]. Gnanasekaran et al. achieved visible light degradation of methyl orange and methylene blue dyes using nanostructured TiO_2/polyaniline nanocomposite [17]. The photo-catalytic performance of TiO_2 has two major problems which are the wide energy gap (3–3.2 eV) that minimize its application to UV region and the fast recombination of charge carriers [18]. TiO_2 is only active in the ultraviolet region (<400 nm), which represents <10% of the overall solar intensity because of its band gap range. Therefore, the light harvesting ability of TiO_2 is very limited [19]. The main challenge in this field is to develop an efficient photo-catalyst TiO_2, which is workable under the visible light region [20]. The present work aims to study photo-catalytic degradation of MB in the presence of nano titanium prepared by sol-gel method with energy band gap that can utilize visible light in the degradation process. The effect of operational conditions such as illumination time, catalyst dose, initial MB concentration and pH on the degradation efficiency of MB was investigated. Characterization of the prepared catalyst was carried out using High resolution transmission electron microscopy (HRTEM), X-ray diffraction (XRD), Bet surface area, UV-visible reflectance and Fourier transform infrared spectroscopy (FTIR). Reaction kinetics was studied using pseudo-first order pattern.

2. Material and methodology

2.1. Materials

Titanium isopropoxide (95%) and palmitic acid were purchased from (Alfa Easer) and (Lobachemie), respectively. Ammonium hydroxide and isopropanol were obtained from (Adwic) and Methylene blue (99%) from (Chemajet). Distilled water had been used through the study. pH was adjusted by HCL and NaOH with concentration of 1 M.

2.2. Synthesis of nano TiO_2

The sol-gel method described by Baker et al. was used to prepare TiO_2 nanoparticles [11]. Palmitic acid (82.7 mmol) and 200 ml of distilled water were stirred in a beaker. Ammonium hydroxide had been added to the solution to achieve homogeneity. Then, a mixture of isopropanol (50 ml) and titanium isopropoxide (16.7 mmol) was prepared and added drop wise to the palmitic acid solution for 2 h and stirred for 12 h. The color of the final mixture became milky white and white colloidal gel was formed. Then, the white colloidal gel was dried at 115°C for 48 h to yield the white powder. Finally, the powder was calcined at 500°C for 3 h.

2.3. Experimental apparatus and procedure

Experimental work was carried out on a photo-reactor apparatus. The schematic of the used reactor is shown in Fig. 1. Various concentrations of MB were prepared using 500 ppm stock solution. The stock solution was prepared by adding 0.5 g of MB in 1 L. The photo-reactor composed of a 250 ml beaker, magnetic stirrer and a 400 W metal halide lamp. The height of the lamp above the beaker was fixed to be 10 cm. A 100 ml of the MB desired concentration was prepared and placed in the reactor and the required catalyst dose was added. Firstly, the solution was stirred in dark for 30 min to achieve adsorption, and then the lamp was switched on to start the photo-catalytic reaction. A sample was taken every 30 min and centrifuged at 4000 rpm for 15 min. The degradation of the dye was monitored by measuring the absorbance on a shimadzu UV-visible spectrophotometer (1601PC, Japan). The absorbance of the dye was measured at wavelength of 660 nm. The concentration of the dye was calculated by using a standard calibration curve for the dye absorbance and its concentrations. Dye removal efficiency X was calculated as shown in Eq. (1) at various time intervals.

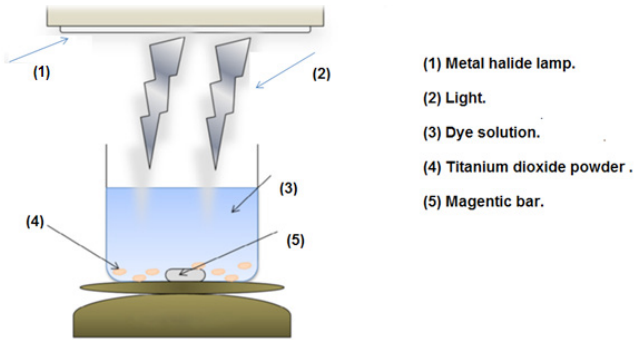

Fig. 1. Schematic of photoreaction experiment setup.

$$X(\%)=\frac{C_o-C}{C_o}*100 \quad (1)$$

where C_o is the initial concentration of dye and C is the concentration of dye at time t.

2.4. Characterization of nano titanium

The morphologies of the synthesized TiO_2 were characterized using transmission electron microscopy (TEM, Joel JEM 2100, Japan) and scanning electron microscope. The X-ray diffraction (XRD) measurements were performed using X-ray diffractometer (Bruker D8 Advanced, German) in the range of 4–80 (2Θ), using a mono-chromatized Cu Kα radiation (λ = 0.154 nm). The functional group of the synthesized TiO_2 was characterized using FTIR Spectroscopy before and after MB degradation (Nicolet is 10, USA). The textural characterization such as surface area, pore volume and pore size distribution of the synthesized photo-catalyst were obtained by N_2 sorption isotherm measurement using (Quanta Chrome Nova 2000, USA). The band gap of synthesized TiO_2 was determined using a UV-Vis-NIR spectrometer (Jasco-V-570, Japan). Scanning electron microscopy (SEM) was employed to examine the surface characteristics of TiO_2 before and after MB degradation.

3. Results and discussion

3.1. Characterization

3.1.1. Morphological analysis

The micrograph of the catalyst is shown in Fig. 2 . The TEM image shows that most of the nanoparticles crystallize are in a cubic morphology. Shadow regions in the picture indicate that the particles may have been agglomerated. Fig. 2 shows that the particle size was found to be in the range of 6.85–14.85 nm, which suggests high surface area of the prepared particles. The SEM images (Figs. 3a, b) demonstrated significant changes in surface topography between TiO_2 before and after MB dye degradation. This change indicated the adsorption of MB dye onto TiO_2 surface, which is of a great importance for the degradation of MB dye.

3.1.2. X-ray diffraction

The phase composition and the crystallite size of the prepared TiO_2 samples were evaluated by the X-ray powder diffraction analysis. Fig. 4 presents the XRD pattern of the calcined TiO_2 powder. It shows sharp and well-defined peaks, indicating good crystallinity of the synthesized material. The peak positions and their relative intensities are consistent with the standard powder diffraction patterns of anatase TiO_2. Since the main peaks appear at 25.37°, 37.4° and 48.1° [21]. This agrees with the JCPDS card (NO: 84-1286) corresponding to anatase TiO_2 which indicates that TiO_2 is tetragonal. The average crystallite size for the TiO_2 nano powder was estimated according to the Scherrer's equation [16]

$$D = \frac{K * \lambda}{\beta * \mathrm{Cos}\,\theta} \quad (2)$$

where K is the Scherrer constant, λ is the X-ray wavelength, β is the peak width at half maximum and θ is the Bragg's diffraction angle.

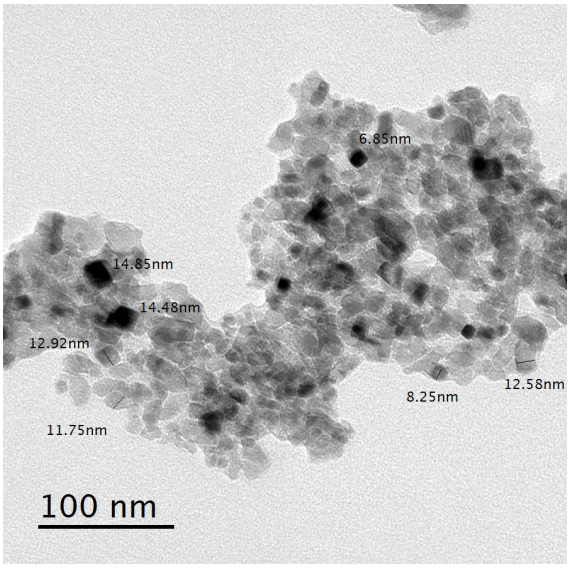

Fig. 2. TEM image of TiO_2 nanoparticles.

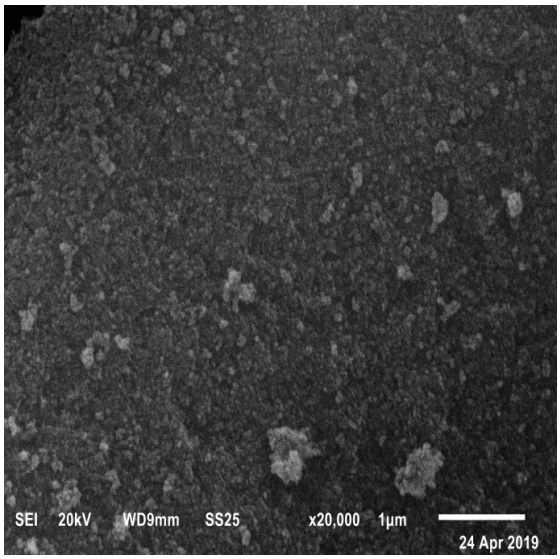

(a)

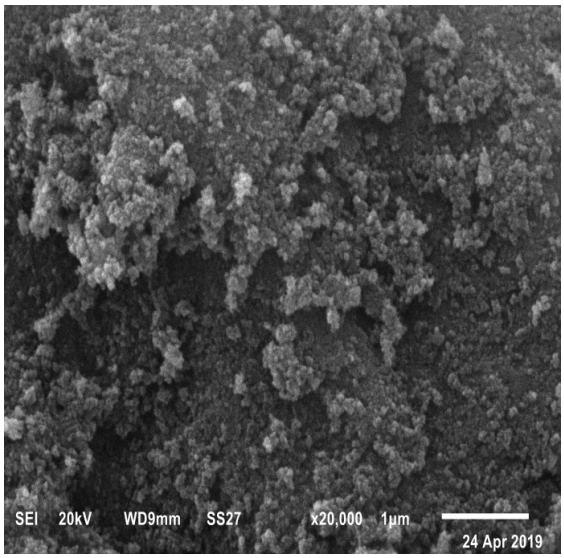

(b)

Fig. 3. SEM images of TiO_2 nanoparticles (a) before degradation and (b) after degradation of MB dye.

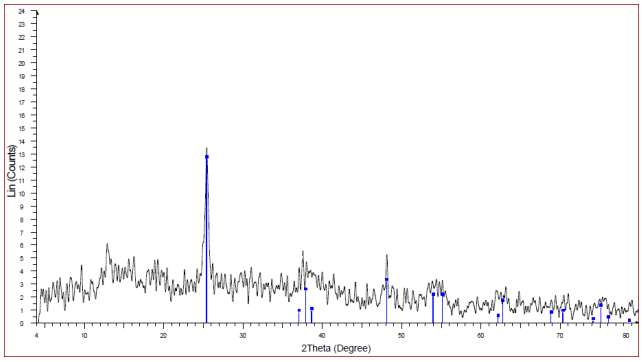

Fig. 4. XRD pattern of prepared TiO_2 nanoparticles.

The average particle size has been determined from the most predominant highest intensity peak and calculated to be 15 nm which is accordance with the results obtained from TEM.

3.1.3. UV-visible reflectance

The band gap energies of the prepared catalysts were calculated via UV-Visible spectroscopy using the Kubelka–Munk function by plotting the graph between $(F(R)\ h\nu)^{1/2}$ on y-axis and hν on x-axis as shown in Fig. 5 .

$$F(R)=\frac{(1-R)^2}{2R} \tag{3}$$

where R is the reflectance and hν = 1240/λ .The band gap value is the intersection of the extrapolating linear portion of $(F(R)\ h\nu)^{1/2}$ versus hν with the x-axis [22]. The band gap energy (Eg) of synthesized TiO_2 nanoparticles was 2.97 eV. Band gap of the semiconductors depends on the particle size [10]. Band gap of the synthesized TiO_2 nanoparticles falls in the visible light region of the electromagnetic spectrum (417.5 nm). This indicates that the photo-catalyst TiO_2 is active under visible light irradiation. Gnanasekaran et al. used nanostructured TiO_2/polyaniline nanocomposite to achieved visible light degradation of methyl orange and methylene blue dyes [17].

3.1.4. FTIR spectroscopy

Fig. 6 shows the FTIR spectra of TiO_2 nanoparticles to identify the functional group. The broad bands observed at 3424 and 3450 cm^{-1} are assigned to the asymmetrical and symmetrical stretching vibrations of hydroxyl group (–OH) and the band appears at 1625 cm^{-1} corresponds to deformation vibration of Ti-OH stretching modes. These bands are evidence of the adsorbed water on the TiO_2 surface [23,24]. The bands observed at 2927 cm^{-1}, 2965 cm^{-1} and 1382 cm^{-1} correspond to the stretching and bending modes of C-H bonds, which come from the residual organic materials in the prepared TiO_2. The band appears at 449 cm^{-1} corresponds to the Ti-O bending mode of TiO_2 [25].The broad bands at 580 cm^{-1} and 650 cm^{-1} after degradation were due to Ti–O bending modes. The band at 804 cm^{-1} appeared after degradation was a result of the Ti-O bond stretching mode of the anatase of the TiO_2 [26,27]. The broad bands at 1026 cm^{-1}, 1099 cm^{-1} and 1261 cm^{-1} after degradation were attributed to C–O stretching vibration. Also the presence of methylene group was confirmed by the appearance of two strong bands at 2962–2856 cm^{-1} after degradation [28]. The results after degradation suggested the new interactions between TiO_2 nanoparticles and methylene blue.

3.1.5. BET surface area

The pore structure and the surface area of the synthesized TiO_2 were investigated by performing N_2 physical adsorption–desorption studies at 77.35 K. N_2 adsorption/desorption isotherm and pore width distributions were obtained as shown in Figs. 7a and b. Synthesized TiO_2 nanoparticles have an average pore radius of 5.267 nm. The multipoint BET specific surface area obtained from the adsorption data at relative pressure (P/P0) of 0.962677 was found to be 79.63 m^2/g. Pore volume for pores with radius less than 26.75 nm at (P/Po) = 0.962677 was .02097 cm^3/g. These results confirmed that the synthesized nanoparticles have high surface area and meso-porosity.

3.2. Comparison between dark and irradiation

Fig. 8 shows the change in dye concentration with operational time for three cases using TiO_2 (1 g/L) in light, using TiO_2 (1g/L) in dark and finally in light without the addition of TiO_2. It is evident that the optimum degradation of MB dye was achieved using TiO_2 in the presence of light. Light activates TiO_2 which leads to the formation of electron and holepairs and produce hydroxyl radical which oxidize the organic matter. TiO_2 in the presence of light achieved dye removal efficiency of 94.9% after 210 min of operational time, compared to 27% degradation of MB dye using TiO_2 in dark. This may be attributed to the fact that TiO_2 adsorption is limited in dark and TiO_2 is not activated due to the absence of light and cannot promote the oxidation of MB dye. In case of operation under light without TiO_2, no significant degradation was attained after 210 min of irradiation time.

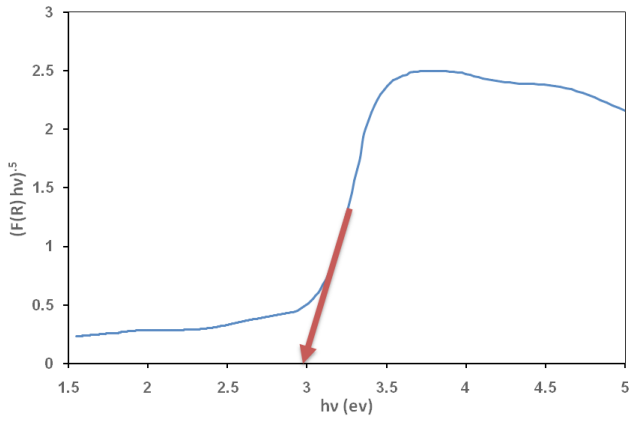

Fig. 5. Band gap calculated by extrapolating the linear portion of $(F(R)\ h\nu)^{1/2}$ versus hν.

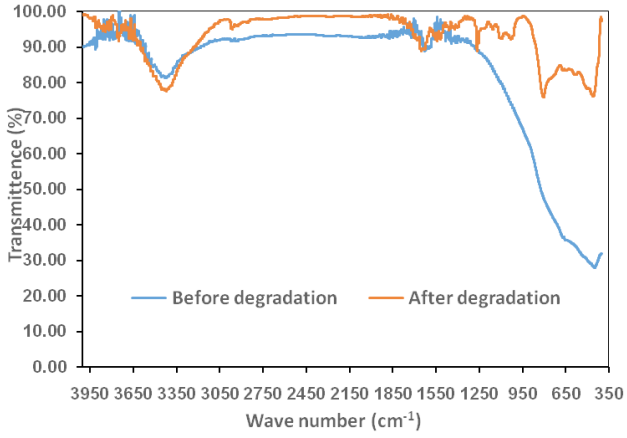

Fig. 6 . FTIR spectrum of TiO_2 nanoparticles before and after MB dye degradation.

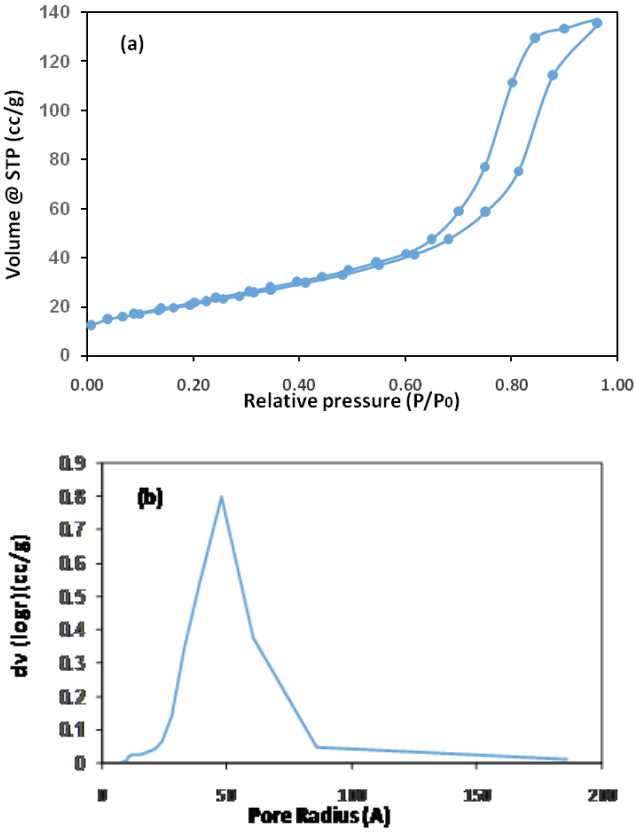

Fig. 7. (a) Nitrogen adsorption–desorption isotherms and (b) pore size distribution of TiO_2 nanoparticles.

3.3. Effect of catalyst dose on the dye removal efficiency

Fig. 9 shows the change of MB concentration with irradiation time using various concentrations of TiO_2 catalyst dose. As the concentration of the catalyst increases from .1 to 1 g/L, the degradation efficiency of MB increases from 72.3% to 94. 9%. It is clear that increasing the catalyst dose increases the number of adsorbed organic molecules and the available active sites for photon absorbance [10]. Therefore, the photo-degradation efficiency of MB increases. MB degradation efficiency increased from 94.9% to 96.9% by increasing the catalyst dose from 1 g/L to 3 g/L, respectively. The results indicated that using a catalyst dose higher than 1 g/L did not improve for the photo-degradation efficiency significantly. The higher catalyst dosage used, the higher solution turbidity occurred, that leads to the reduction of light penetration by the scattering effect [29]. Another reason may be related to the aggregation of particles at high catalyst dose [30], which results in the reduction of active surface available for adsorbing of MB and light radiation.

3.4. Effect of initial MB concentration on the removal efficiency

Fig. 10 shows the effect of initial MB concentration varies from 2.5 to 25 mg/L on the removal efficiency using a catalyst dosage of 1 g/L at pH value of 7±0.5. At low dye concentration the light goes easily through the solution to irradiate the TiO_2, so that the photonic efficiency increases

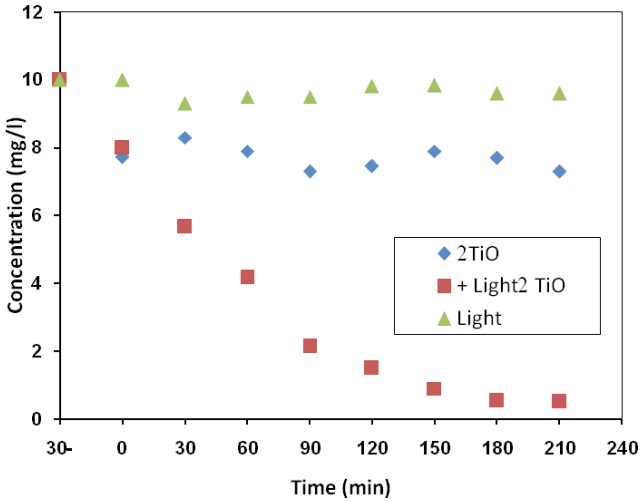

Fig. 8. Effect of light and TiO_2 nanoparticles on MB degradation efficiency, MB dye concentration = 10 mg/L, catalyst dose = 1 g/L, pH = 7±0.5.

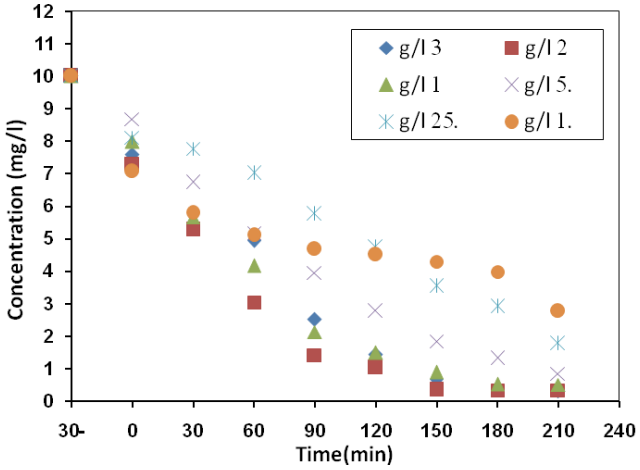

Fig. 9. Effect of catalyst dose on the photo-degradation efficiency, MB dye concentration = 10 mg/L, pH = 7±0.5.

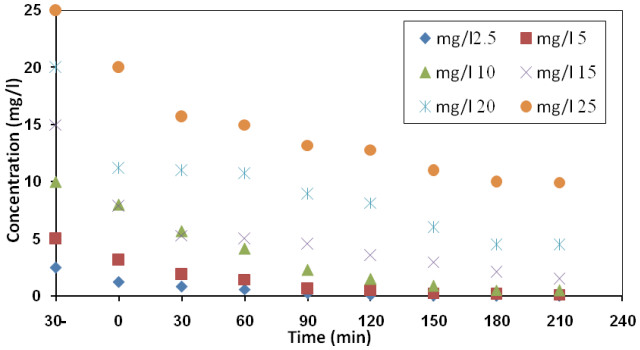

Fig. 10. Effect of dye concentration on photo-degradation efficiency, catalyst dose = 1 g/L, pH = 7±0.5.

resulting in higher photo-degradation efficiency. Increasing the dye initial concentration from 2.5 mg /L to 25 mg/L decreased the photo-degradation efficiency from 98% to 60%, respectively. This may be related to the number of adsorbed molecules of MB increased on the surface of TiO_2, which reduced the active sites available for hydroxyl ions adsorption and reduced the generation of hydroxyl radicals [31,32]. Furthermore, as the dye concentration increased, the photon get intercepted before they can reach the catalyst surface, hence the adsorption of the photons by the catalyst decreased, and consequently the catalyst surface will not be activated and MB degradation efficiency will be reduced [33,27]. This study achieved 96.97% removal of MB in 210 min compared to 91% removal of MB in 420 min achieved by Bin Mukhlish et al. [34] under the same operational conditions which indicates the improvement of nano titanium degradation efficiency.

3.5. Effect of pH on the removal efficiency

The solution pH affects the photo-degradation efficiency of various pollutants [35,36]. The effect of pH on the photo-degradation efficiency of MB was studied by changing solution pH from 3 to 11. The pH of the solution was not controlled during the course of the reaction and adjusted before irradiation using HCL and NaOH with concentration of 1 M. Fig. 11 shows that the degradation efficiency increases with increasing the pH from 3 to 11. The photo-degradation efficiency increased from 18% to 96% by raising the pH from 3 to 11, respectively. Alqadami et al. [1] has similar results using MOF nanocomposite for MB adsorption. The pH affects not only the dye dissociation but also the surface properties of the photo-catalyst and OH radical formation [6]. The effect of pH on surface charge can be described according to the following equations

$$pH \prec pHp_{zc} : TiOH + H^+ \rightarrow TiOH_2^+ \quad (4)$$

$$pH \succ pHp_{zc} : TiOH + oH^- \rightarrow TiO^- + H_2O \quad (5)$$

The pH of the point of zero charge (pHp_{zc}) of TiO_2 is reported to be equal to 6.25 [37,38]. TiO_2 surface has a positive charge at solution pH below the pHp_{zc} and has a net negative charge at solution pH above the pHp_{zc} [18]. For pH equal to 3, the Cl^- anions have been adsorbed on the surface of TiO_2 which leads to a competition between the adsorption of the Cl^- anions and the dye on the TiO_2 surface [39]. This phenomenon reduces the photo-catalytic activity. However, at the pH value of 5, the quantity of Cl^- anions is lower than the previous case, so that the degradation efficiency increases [18]. At higher pH, TiO_2 becomes negatively charged. Since MB is a cationic dye [40], this increases the adsorption of MB into TiO_2 and consequently increases the degradation rate of MB.

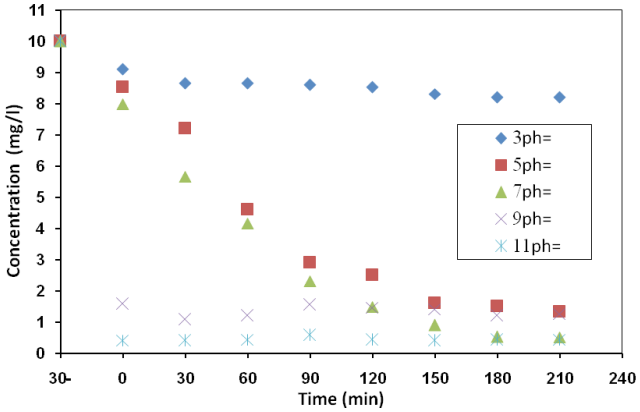

Fig. 11. Effect of pH on photo-degradation efficiency, catalyst dose = 1 g/L, initial dye concentration = 10 mg/L.

3.6 .Kinetics of photocatalytic degradation of MB

The degradation rate for MB was calculated using Langmuir–Hinshelwood model expressed as follow [41,42]:

$$r = \frac{K_r K_{ad} c}{1 + K_{ad} c} \quad (6)$$

where r is the degradation rate, c is the reactant concentration at time (t), k_r is the rate constant and K_{ad} is the adsorption equilibrium constant. In photo-catalysis where the adsorption is relatively weak like and/or the reactant concentration is low, Eq. (6) can be simplified to the pseudo- first order kinetics with an apparent first-order rate constant k_{app} [41]:

$$Ln\left(\frac{C_o}{C}\right) = K_r K_{ad} t = k_{app} t \quad (7)$$

where C_o is the initial concentration of MB and C is the concentration of MB remaining after time t. To study the kinetics of photo-degradation of MB, experiments were conducted using TiO_2 dose of 1 g/L, irradiation time of 210 min and pH = 7±0.5. The concentration of MB dye after 30 min in the dark was considered to be the initial concentration for kinetics analysis. Fig. 12 shows the model equation and experimental data at various solution concentrations. Table 1 shows the fitting parameter and the correlation coefficient R^2 for the pseudo-first order kinetics. It was demon-

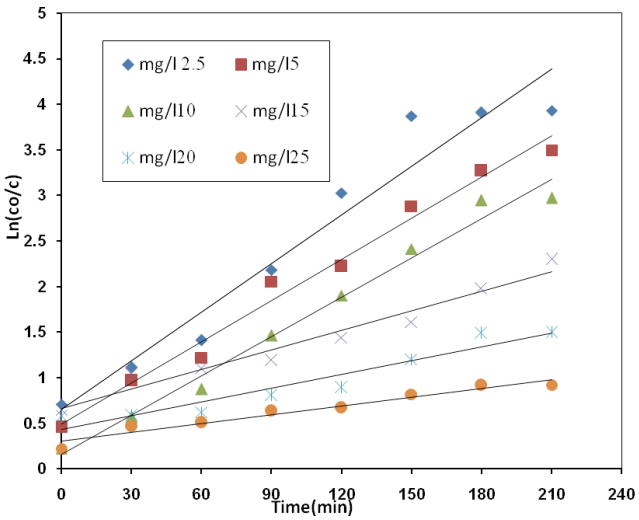

Fig. 12. Kinetics analysis of MB degradation, catalyst dose = 1 g/L, pH = 7±0.5.

Table 1
Pseudo-first order parameters and the correlation coefficient at various dye concentrations

Initial concentration (mg/l)	K_{app} (min^{-}1)	R^2
2.5	0.0178	0.9459
5	0.0151	0.9852
10	0.0144	0.9852
15	0.0072	0.9611
20	0.005	0.9199
25	0.0032	0.9519

strated that the results were validated by pseudo-first order. It was found that as the initial dye concentrations increased, the reaction rate decreased. The possible explanation for this behavior can be as the initial dye concentration increases, the path length of photons entering the solution decreases [43-45] but for low dye concentrations the reverse effect was observed. In addition, at higher dye concentrations, the dye molecules may absorb a significant amount of light rather than the catalyst and this also may reduce the catalytic efficiency [46]. Neppolian et al. obtained similar results using TiO_2 photo-catalyst and solar light for the degradation of the commercial textile dyes [47].

4. Conclusions

In this study, photo-catalytic experiments were carried out under various operation conditions using synthesized nano TiO_2 for MB degradation. MB was successfully degraded by using the synthesized nano TiO_2 in visible light depending on the band gap energy calculations. Morphological analysis suggests high surface area of the prepared particles. The average particle size of TiO_2 was 15 nm. Band gap of the synthesized TiO_2 falls in the visible light region, which indicates the activation of TiO_2 under visible light irradiation. SEM and FTIR before and after degradation demonstrated the interaction between MB dye and TiO_2. The photo-catalytic degradation efficiency of MB increased with increasing the illumination time. It was also noted that the MB removal efficiency was inversely related to the feed MB initial concentration. The highest MB photo-catalytic degradation was achieved at alkaline media. The data was successfully validated by the Langmuir–Hinshelwood pseudo-first order kinetic model.

Symbols

C_0 — Initial concentration of dye (mg/l).
C — Dye concentration at time t (mg/l).
X% — Dye removal efficiency (%).
D — The average crystallite size for the TiO_2 nano powder.
K — The Scherrer constant.
λ — The X-ray wavelength.
β — The peak width at half maximum.
θ — The Bragg's diffraction angle.
r — The degradation rate.
k_r — Reaction rate constant.
k_{ad} — Equilibrium adsorption coefficient.
k_{app} — Apparent pseudo-first-order rate constant.

References

[1] A.A. Alqadami, Mu. Naushad, Z.A. Alothman, T. Ahamad, Adsorptive performance of MOF nanocomposite for methylene blue and malachite green dyes: Kinetics, isotherm and mechanism, J. Environ. Manage., 223 (2018) 29–36.
[2] D. Pathania, D. Gupta, A.H. Al-Muhtaseb, G. Sharma, A. Kumar, M. Naushad, T. Ahamad, S.M. Alshehri, Photocatalytic degradation of highly toxic dyes using chitosan-g poly(acrylamide)/ZnS in presence of solar irradiation, J. Photochem. Photobiol. A Chem., 329 (2016) 61–68.
[3] E. Daneshvar, A. Vazirzadeh, A. Niazi, M. Kousha, Mu. Naushad, A. Bhatnagar, Desorption of methylene blue dye from brown macroalga: effects of operating parameters, isotherm study and kinetic modeling, J. Cleaner Prod., 152 (2017) 443–453.
[4] I. Arslam, I.A. Balcioglou, T. Tuhkanen, D. Bahnemann, Photochemical and photocatalytic detoxification of reactive dye bath wastewater by the Fenton's reagent and novel TiO_2 powders, J. Environ. Eng., 126 (2000) 903–911.
[5] N. Stock, J. Peller, K. Vinodgopal, P.V. Kamat, Combinative sonolysis and photocatalysis for textile dye degradation, Environ. Sci. Technol., 34 (2000) 1747–1750.
[6] K. Hayat, M.A. Gondal , M.M. Khaled, Z.H. Yamani, S. Ahmed, Laser induced photo catalytic degradation of hazardous dye (Safranin-O) using self-synthesized nano crystalline WO_3, J. Hazard. Mater., 186 (2011) 1226–1233.
[7] G. Sharma, Mu. Naushad, A. Kumar, S. Rana, S. Sharma, A. Bhatnagar, F.J. Stadler, A.A. Ghfar, M.R. Khan, Efficient removal of coomassie brilliant blue R-250 dye using starch/poly (alginic acid-cl-acrylamide) nanohydrogel, Process Safety Environ. Protect., 109 (2017) 301–310.
[8] C.G. Silva, J.L. Faria, Photochemical and photocatalytic degradation of an azo dye in aqueous solution by UV irradiation, J. Photochem. Photobiol. A: Chem., 155 (2003) 133–143.
[9] D. Dvoranova, V. Brezova, M. Mazur, M.A. Malati, Investigations of metal-dopedtitanium dioxide photocatalysts, Appl. Catal. B: Environ., 37 (2002) 91–105.
[10] A. Amalraj, A. Pius, Photocatalytic degradation of monocrotophos and chlorpyrifos in aqueous solution using TiO_2 under UV radiation, J. Water Process Eng., 7 (2015) 94–101.
[11] P.V. Bakre, P.S. Volvoikar, A.A. Vernekar, S.G. Tilve, Influence of acid chain length on the properties of TiO_2 prepared by sol-gel method and LC-MS studies of methylene blue photodegradation, J. Colloid Interface Sci., 474 (2016) 58–67.
[12] K. Pirkanniemi, M. Sillanpaa, Heterogeneous water phase catalysis as an environmental application: a review, Chemosphere, 48 (2002) 1047–1060.
[13] T. Jr. Yates, T.L. Thompson, Surface science studies of the photoactivation ofTiO_2-new photochemical processes, Chem. Rev., 106 (2006) 4428–4453.
[14] A. Fujishima, X. Zhang, Titanium dioxide photocatalysis: present situation and future approaches, C.R. Chimie., 9 (2006) 750–760.
[15] A. Alinsafi, F. Evenou, E.M. Abdulkarim, M.N. Pons, O. Zahraa, A. Benhammou, A. Yaacoubi, A. Nejmeddine, Treatment of textile industry wastewater by supported photocatalysis, Dyes Pigs., 74 (2007) 439–445.
[16] J.A.I. Joice, T. Sivakumar , R. Ramakrishnan , G. Ramya, K.P.S. Prasad, D.A. Selvan, Visible active metal decorated titania catalysts for the photocatalytic degradation of Amidoblack-10B, Chem. Eng. J., 210 (2012) 385–397.
[17] L. Gnanasekaran, R. Hemamalini, Mu Naushad, Efficient photocatalytic degradation of toxic dyes using nanostructured TiO_2/polyaniline nanocomposite, Desal. Water Treat., 108 (2018) 322–328.
[18] M. Khraisheh, L. Wub, A.H. Al-Muhtaseb, A.B. Albadarin , G.M. Walker, Phenol degradation by powdered metal ion modified titanium dioxide photocatalysts, Chem. Eng. J., 213 (2012) 125–134.

[19] H. Sun, S. Wang, H. Ang, M.O. Tade, Q. Li, Halogen element modified titanium dioxide for visible light photocatalysis, Chem. Eng. J., 162 (2010) 437–447.
[20] D. Ravelli, D. Dondib, M. Fagnonia, A. Albinia, Titanium dioxide photocatalysis: an assessment of the environmental compatibility for the case of the functionalization of heterocyclics, Appl. Catal. B: Environ., 99 (2010) 442–447.
[21] J. Ananpattarachai, P. Kajitvichyanukul, S. Seraphin, Visible light absorption ability and photocatalytic oxidation activity of various interstitial N-doped TiO_2 prepared from different nitrogen dopants, J. Hazard. Mater., 168 (2009) 253–261.
[22] Y. Niu , M. Xing, J. Zhang, B. Tian, Visible light activated sulfur and iron co-doped TiO_2 photocatalyst for the photocatalytic degradation of phenol, Catal. Today, 201 (2013) 159–166.
[23] C.E. Zubieta, P.V. Messina, P.C. Schulz, Photocatalytic degradation of acridine dyes using anatase and rutile TiO_2, J. Environ. Manage., 101 (2012) 1–6.
[24] T. Bezrodna, G. Puchkovska, V. Shymanosvska, J. Baran, H. Ratajczak, IR analysis of H-bonded H_2O on the pure TiO_2 surface, J. Mol. Struct., 700 (2004) 175–181.
[25] D. Wang, L. Xiao, Q. Luo, X. Li, J. An, Y. Duan, Highly efficient visible light TiO_2 photocatalyst prepared by sol–gel method at temperatures lower than 300°C, J. Hazard. Mater., 192 (2011) 150–159.
[26] N. Daneshvar, D. Salari, A.R. Khataee, Photocatalytic degradation of azo dye acid red 14 in water: investigation of the effect of operational parameters, J. Photochem. Photobiol. A: Chem., 157 (2003) 111–116.
[27] M.V. Shankar, S. Anandan, N. Venkatachalam, B. Arabindoo, V. Murugesan, Novel thin-film reactor for photocatalytic degradation of pesticides in aqueous solutions, J. Chem. Technol. Biotechnol., 79 (2004) 1258–1279.
[28] Mu. Naushad, T. Ahamad, G. Sharma, A.H. Al-Muhtaseb, A.B. Albadarin, M.M. Alam, Z.A. ALOthman, S.M. Alshehri, A.A. Ghfar, Synthesis and characterization of a new starch/SnO_2 nanocomposite for efficient adsorption of toxic Hg^{2+} metal ion, Chem. Eng. J., 300 (2016) 306–316.
[29] L. Wei , C. Shifu, Z. Wei, Z. Sujuan, Titanium dioxide mediated photocatalytic degradation of methamidophos in aqueous phase, J. Hazard. Mater., 164 (2009) 154–160.
[30] B. Neppolian, H.C. Choi, S. Sakthivel, B. Arabindoo, V. Murugesan, Solar lightinduced and TiO_2 assisted degradation of textile dye reactive blue 4, Chemosphere, 46 (2002) 1173–1181.
[28] Y. Liu , Y. Ohko, R. Zhang, Y. Yang, Z. Zhang, Degradation of malachite green on Pd/WO_3 photocatalysts under simulated solar light, J. Hazard. Mater., 184 (2010) 386–391.
[31] C.S. Lu, Y.T. Wu, F.D. Mai, W.S. Chung, C.W. Wu, W.Y. Lin, C.C. Chen, Degradation efficiencies and mechanisms of the ZnO-mediated photocatalytic degradation of Basic Blue 11 under visible light irradiation, J. Mol. Catal. A: Chem., 310 (2009) 159–165.
[32] M.A. Rauf, S.S. Ashraf, Fundamental principles and application of heterogeneous photocatalytic degradation of dyes in solution, Chem. Eng. J., 151 (2009) 10–18.
[33] S. Chakrabarti, B.K. Dutta, Photocatalytic degradation of model textiledyes in wastewater using ZnO as semiconductor catalyst, J. Hazard. Mater. B, 112 (2004) 269–278.
[34] M.Z. Bin Mukhlish, F. Najnin, M.M. Rahman, M.J. Uddin, Photocatalytic degradation of different dyes using TiO_2 with high surface area: a kinetic study, J. Sci. Res., 5 (2013) 301–314.
[35] S. Sakthivel, B. Neppolian, M.V. Shankar, B. Arabindoo, M. Palanichamy, V. Murugesan, Solar photocatalytic degradation of azo dye: comparison of photocatalytic efficiency of ZnO and TiO_2, Sol. Energy Mater. Sol. Cells., 77 (2003) 65–82.
[36] C. Lizama, J. Freer, J. Baeza, H.D. Mansilla, Optimized photodegradation ofReactive Blue 19 on TiO_2 and ZnO suspensions, Catal. Today, 76 (2002) 235–246.
[37] J. Fenoll, P. Flores, P. Hellı´n, C.M. Martı´nez, S. Navarro, Photodegradation of eight miscellaneous pesticides in drinking water after treatment with semiconductor materials under sunlight at pilot plant scale, Chem. Eng. J., 204–206 (2012) 54–64.
[38] S. Ahmed, M.G. Rasul, R. Brown, M.A. Hashib, Influence of parameters on the heterogeneous photocatalytic degradation of pesticides and phenolic contaminants in wastewater: A short review, J. Environ. Manage., 92 (2011) 311–330.
[39] D. Chen, A.K. Ray, Photodegradation kinetics of 4-nitrophenol in TiO_2 suspension, Water Res. 32 (1998) 143–157.
[40] R.S. Dariani, A. Esmaeili, A. Mortezaali, S. Dehghanpour, Photocatalytic reaction and degradation of methylene blue on TiO_2 nano-sized particles , Optik, 127 (2016) 7143–7154.
[41] Y.A. Shaban, M.A. El Sayed, A.A. El Maradny, R.K. AlFarawati, M.I. Al Zobidi, Photocatalytic degradation of phenol in natural seawater using visible light active carbon modified (CM) n-TiO_2 nanoparticles under UV light and natural sunlight illuminations, Chemosphere, 91 (2013) 307–313.
[42] Ö. Kartal, M. Erol, H. Oguz, Photocatalytic destruction of phenol by TiO_2 powders, Chem. Eng., 24 (2001) 645–649.
[43] E. Bizani, K. Fytianos, I. Poulios, V. Tsiridis, Photocatalytic decolorization and degradation of dye solutions and wastewaters in the presence of titanium dioxide, J. Hazard. Mater., 136 (2006) 85–94.
[44] J. Zhao, T. Wu, K. Wu, K. Oikawa, H. Hidaka, N. Serpone, Photo assisted degradation of dye pollutants 3: evidence for the need for substrate adsorption on TiO_2 particles, Environ. Sci. Technol., 32 (1998) 2394–2400.
[45] R.J. Davis, J.L. Gainer, G.O. Neal, I.W. Wu, Photocatalytic decolorization of wastewater dyes, Water Environ. Res., 66 (1994) 50–53.
[46] A. Mills, R.H. Davis, D. Worsely, Water purification by semiconductor photocatalysis, Chem. Soc. Rev., 22 (1993) 417–425.
[47] B. Neppolian, H.C. Choi, S. Sakthivel, B. Arabindoo, V. Murugesan, Solar/UV induced photocatalytic degradation of three commercial textile dyes, J. Hazard. Mater. B, 89 (2002) 303–317.